



ELSEVIER

Contents lists available at ScienceDirect

## Computer Networks

journal homepage: [www.elsevier.com/locate/comnet](http://www.elsevier.com/locate/comnet)

## Performance analysis of a delay tolerant application for herd localization

Nelson I. Dopico\*, Álvaro Gutiérrez, Santiago Zazo

ETSI Telecomunicación, Universidad Politécnica de Madrid, Avda. Complutense 30, 28040 Madrid, Spain

## ARTICLE INFO

## Article history:

Received 29 July 2010

Received in revised form 10 November 2010

Accepted 14 January 2011

Available online xxx

Responsible Editor: N. Rahnvard

## Keywords:

Localization

Wireless sensor networks

Delay tolerant networks

Ubiquitous systems

## ABSTRACT

Target localization feasibility may depend on economical and environmental reasons and not only on technical ones as it is considered frequently. Thus, equipment costs may exceed the target value and system operation/deployment may demand tasks which collide with environmental regulations or simply do not pay off if they are compared to the gained advantage. Different solutions have been deployed for animal localization which may require satellite transmitters or employ solar energy as a workaround for power supply constraints. However, the former can turn out to be expensive and the latter useless in latitudes with limited sunlight. We analyze the performance of a localization system which aims to overcome the aforementioned issues in herding environments. Different kinds of nodes along with flexible duty cycles leverage the system adaptiveness, meeting users' needs and complying with different environmental policies. Our analyses are based on real tests and combinations of such modeling with simulations. As a consequence of the system flexibility, the analyzed configurations exhibit wide ranges for magnitudes such as localization delay and localization events.

© 2011 Elsevier B.V. All rights reserved.

## 1. Introduction

Years ago, Kahn et al. [1] foresaw a future with versatile sensor nodes all around capable to operate autonomously with little consumption. Over the last decade major efforts with different approaches have been devoted to achieve such goals. Thus, most works have focused on theoretical analysis, many less on studies with real traces and even less with equipment on real operation which combined the two previous at the same time. Kahn aimed at self powered nodes consuming around one Joule per day and considered the possibility of integrating optical communications rather than radio frequency to link the node to a base-station transceiver. Applications ranging from biological to planetary research were pointed out as well.

Delay tolerant networks [2,3] are a fresh research area and standardization is still a work in progress which feedbacks from simulations, pilot deployments and a series of

research initiatives. DTNs enable data transfer when (generally) mobile nodes are connected only intermittently. Such intermittent connectivity can be a result of mobility, power management, wireless range, sparsity or malicious attacks [4]. DTN was coined as a term after the architecture for the interplanetary internet (IPN) project [5]. By 2003, the time that the first draft of RFC 4838 [6] was published, it was suggested to extend the concept of IPN to other kinds of networks [2]. That vision along with researchers' growing interest in wireless sensor networks (WSNs) and other exotic ones boosted the work of the research community which falls under the term DTN.

The work presented in the current paper is part of the project networking for communications challenged communities [7]. The project joins research and technical knowledge to support threatened communities by providing them with modern facilities (such as networked appliances and Internet access) to maintain their culture and lifestyle and thus avoiding, as much as possible, the emigration to cities with the negative consequences regarding their integration and lost of culture and lifestyle. Our team is facing the challenge of providing these communities

\* Corresponding author. Tel.: +34 91 5495700x4006.

E-mail addresses: [nelson@gaps.ssr.upm.es](mailto:nelson@gaps.ssr.upm.es) (N.I. Dopico), [aguti@etsit.upm.es](mailto:aguti@etsit.upm.es) (Á. Gutiérrez), [santiago@gaps.ssr.upm.es](mailto:santiago@gaps.ssr.upm.es) (S. Zazo).

with a ubiquitous system which enables them to monitor their herds in several scenarios over the year [8]. In such context, herders are not required to be permanently with their herds and at the same time the system facilitates their monitoring when they are roaming across wide areas without fences or barriers.

Ubiquitous networking (like our system operation) is often referred to in terms of traditional mobile telephony and wireless networks and is generally meant as enabling applications to operate wherever individuals go [9]. While this is a very fine goal, in most of today's ubiquitous networking projects, ubiquitous is confined to a very narrow area that has a superior connectivity [10]. However, the term 'ubiquitous' means existing or being everywhere at the same time: constantly encountered. 'Everywhere' means that truly ubiquitous computing must extend to all those places that are outside the region of dense networking capability such as communications-challenged communities. Areas may be considered challenged for a variety of reasons, for example, because even satellites do not cover the area, because of war and other disastrous scenarios, because power lines do not reach there yet, or because governmental policies prevent any access [11]. Another use of the term ubiquitous involves the development of appliances that have computing and networking embedded. In this context it means that computing capabilities need to become pervasive within all spheres of people's lives, including both work and leisure, so that their lives are improved. The goals of pervasive computing involve making the lives of people living in remote areas easier by means of the use of networked appliances and other devices. Pervasive computing does not differentiate between indoors or outdoors, and it should not differentiate between communications-rich areas and communications-challenged areas.

One of the extensions of pervasive computing into outdoors involves adding sensor network capabilities that aid herders to track their herds without needing to physically follow their herds. For example, tracking reindeer in winter is a very intensive labor and interferes with herders' capability to do other tasks or care for their families. Adding the capability to track reindeers and relay the information back to their mobile devices would do a lot to improve the economic opportunities for residents of marginal communities. As an example, a semi-nomadic population cannot simultaneously participate in the modern fixed location school system while living a traditional life. Using pervasive technology to facilitate certain traditional tasks will bring a form of harmony between the modern and the traditional, and will do much to decrease the contradictions and stress of the semi-nomadic life. Making people's lives easier – as this introduction is outlining – comprises other consequences or implications. One of them is a basis of pervasive computing, i.e. recognizing that technology must serve a population's culture rather than fitting it by forcing into the prevailing technological box as it would happen with semi-nomadic populations like the aforementioned herders.

The reindeer herds, that are the basis of traditional economic activity in the Sami region, roam freely over very wide areas. This paper presents a cost-effective way to

monitor both the localization and other information regarding herds and individual animals which can be combined with other delay-tolerant communication networks in order to integrate more smoothly in users' lives. This is challenging both from the point of view of wide areas to be covered and the need to power any animal mounted equipment over extended periods during which solar power would be unavailable.

Although animal localization is technically feasible for some time now as GPS devices are in use since the 90s, our system has been designed to be low cost, adaptive to different requirements and scenarios and environmentally friendly [8]. Other systems may become unfeasible due to the cost per head of herd or because of the environmental impact of lost or damaged batteries. Some of them make use of satellites which locate the animal position [12]. They have been widely used in turtle [13], duck [14] or whale [15] tracking. However, its use is extremely expensive and requires all the satellite transmitters on the animals to be updated in the satellite database. Other approaches make use of storage systems based on solar energy as environmental energy source [16,17]. Some of these implementations have been used for animal tracking, as in the *zebranet* project [18] or the *Turtlenet* project [19]. However, solar energy is severely limited for latitudes where daily sunlight may be short in some seasons or the irradiance is not enough to power the system. To deal with solar energy restrictions, other techniques have been studied. In [20], the authors describe a system which takes advantage of human motion and obtains enough energy for transmitting information. However, the communication is based on a transmitter which does not allow reading distances of more than just a few meters. In [21], the authors follow the same principle by taking advantage of finger motion. A piezo-electric system based on a push button is presented in [22]. Other strategies make use of wind energy [23] or radio frequency energy [24]. However, while the former are not useful for animal tracking systems because animals avoid wind flows, the latter suffer from poor emission ranges which make the system unsuitable. Therefore, with the development of a new system, we try to avoid most of the problems aforementioned.

The current stage of our work is based on previous milestones such as the design and test of the equipment along with field-test deployments which enabled us to model the behavior of every component mounted on reindeers – they are the intended herd to be tracked. However, it is a general purpose system which can be mounted on different herds that humans may consider susceptible to be tracked for any reason as it will be shown later because of its flexibility, adaptiveness and scalability. Based on such modeling and a customized simulator, different set-ups have been studied in order to understand the relationships between the magnitudes on study and the system characteristics and tuning. With the outcomes presented in this paper we expect to adjust better our system to a number of scenarios regarding the challenge we are facing.

Our primary goal is to roughly track animal movements in challenged areas at a very low cost and to reduce the environmental impact with unattended operation. Animal movements do not need to be accurately tracked like an

on-board regular GPS device would be expected to do continuously, but enough to monitor their presence in a certain area a number of times per day. In this way, a herder may know where the herd is, if any animal has left or where it was lately around. Cost is a key factor since this system aims at becoming part of day-to-day life in a regular herder's work whose herd can be composed of up to thousands of cattle, therefore any extra cost might make it easily unprofitable. As any system deployed in natural environments, environmental impact plays a relevant role and should be minimized in such a way that it can be considered practically negligible, especially if we allow for restrictive governmental policies and the fact that the project is targeted to sustaining a traditional lifestyle in a natural environment rather than creating any new pollution source.

Compared to smart dust by Kahn and DTNs, our system integrates characteristics of both. On one hand, nodes are designed to operate with different roles so that – for most – power consumption may not comprise any battery replacement or even a single battery as an intermediate accumulator. On the other hand, network connectivity changes depending on herd mobility and their transmission pattern, therefore the whole system is a paradigm of a DTN.

Better insight of the network operation and architecture can be obtained from Section 2. A description on the simulator, its characteristics and simulation assumptions can be found in Section 3. Section 4 details the experiments performed and discusses the results regarding three metrics: localization events, localization error and localization delay. Finally, Section 5 summarizes the main results and concludes the article.

## 2. Network architecture

The network architecture proposed is made up of three different elements: primary nodes, secondary nodes and base stations (see Fig. 2).<sup>1</sup> The equipment described hereafter is designed and manufactured specifically for our application. However, components are regular ones which any individual may find from any supplier. Primary and secondary nodes are mounted on animals and therefore are mobile nodes, while base stations are static nodes.

Secondary nodes are the simplest elements in the network. They take kinetic energy (see Fig. 1) from animal movements which produce just enough power to create and broadcast a unique identification (ID) to the environment without confirmation of its reception. If a primary node is within the transmission range, it receives and stores the transmitted ID.

Moreover, primary nodes are able to obtain their global position thanks to a global positioning system (GPS) which can be switched on and off depending on the final application needs. Therefore, a primary node, which receives a transmission from a secondary node, approximates the aforementioned secondary node's position through its own location. While the primary node is moving in the



Fig. 1. Kinetic generator in secondary nodes.

environment, it creates a table with the different secondary-node IDs received, their approximated position and the time when the transmission was produced. When a primary node enters within the base-station communication range, it transmits all the information acquired from the secondary nodes along with its own trajectory information. A base station is a static battery-powered node which has access to the Internet and is able to offer data to a final monitoring system. Therefore, once a base station receives data dumped by a primary node, it sends it to the monitoring system. Such monitoring system is expected to receive information from different base stations, hence it will merge all the information and provide it to the end user.

Thanks to the aforementioned operation, the final system has information about position estimates of primary and secondary nodes. Therefore, it will be able to reconstruct the movements carried out by different animals. Note that such reconstruction is an approximation of the actual trajectories followed by individuals, as a consequence of the stochastic transmission of secondary nodes, the probabilistic reception of the primary nodes and the discretization of the GPS readings. As already depicted, the system provides a network architecture to monitor animals in outdoor environments. Nonetheless, in order to work correctly on a specific and real application, some parameters such as the time that the primary nodes are listening to the secondary nodes, the GPS duty-cycle, the ratio between primary and secondary nodes and the base-station density, among others, must be defined for each specific application. Because secondary nodes are non-battery powered, simpler and cheaper than primary nodes, designers' goal should be to reduce the number of primary nodes and base stations in favor of secondary nodes.

Radio links operate in two different bands. Secondary-primary links modulate their information with frequency shift keying (FSK) in the 433 MHz ISM band and a data rate of 4.16 Kbps. Primary-base station links operate in the 166 MHz ISM band with FSK as well, but are able to reach up to 200 Kbps.

### 2.1. Preliminary experiments

Different experiments have been run to characterize and validate system's localization and communication capabilities.

A first experiment was developed in an obstacle-free environment with one secondary and one primary node to test the stochastic secondary-primary node radio link. We observed that for short distances (less than 20 m) all

<sup>1</sup> For a thorough description of the system see [8].

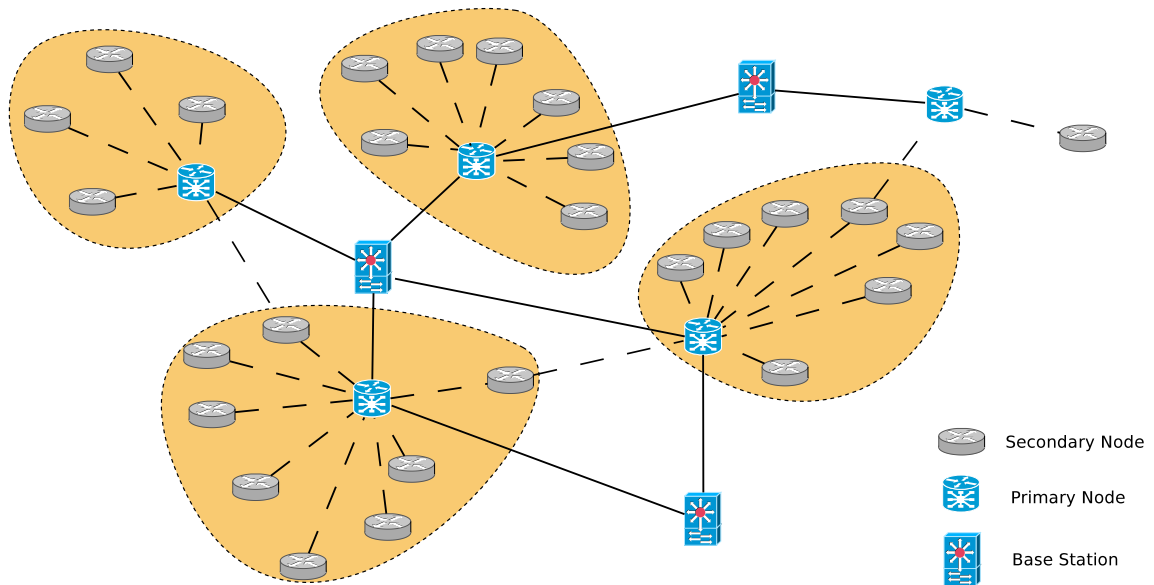


Fig. 2. Network architecture.

the frames transmitted arrived correctly at the primary node. When the emitter was moved away from the receiver, some frames were not received and got lost. Only 30% of the frames arrived at the receiver at 100 m and no frame were received at larger distances. Moreover, we observed that after 30 m some of the frames received were not correctly decoded, with a maximum error of 40% when the nodes were at their maximum transmission range.

Another experiment was developed with a primary node and a base station node in an obstacle-free environment to analyze the primary-base station radio link and the implementation of a specific protocol over it. The primary-base station radio link implements a communication protocol which allows for collisions. Therefore, all the frames transmitted by the primary node were received by the base station if it was within the communication range. However, because of the distance, some messages got lost and the primary node must retransmit them until it received an acknowledgment from the base station.

An experiment involving the GPS was carried out to estimate the time required for the GPS to obtain both current time and position. The selected GPS module navigation device is able to provide current GMT time, latitude and longitude. Device capabilities were tested upon a cold start, which means such device is switched on after being off for a long period. On a cold start, a GPS device needs to find out satellites' position to locate itself and consequently the first action it performs is finding the satellite connection and current time. Typically, from 5 to 20 s are needed for timing acquisition. After this period, the GPS device obtains satellites' positions and once different satellites have been located, the GPS device is able to determine its own location. A period of 2 min on average is needed for localization after a cold start. GPS updates are then performed every second if the module is not completely switched off.

Finally, a simple proof-of-concept study of the network was performed to validate a first version of the system on live animals. The overall idea for an animal test was to check:

- if the animal movements were able to swing the generator to produce enough energy for the ID transmission and
- if the node size and dimensions were feasible at least for some mammals

Tests were performed on a dog and a reindeer. The best place for the secondary node location turned out to be the animal's neck – Fig. 3. As animals move their neck (e.g. on search for food on the ground) the generator is swung. The neck was selected because, to best take advantage of the energy, the generator needs to be swung from end to end (see [8]).

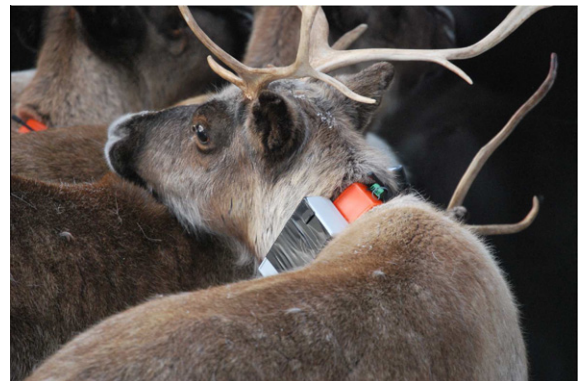


Fig. 3. Collar with primary and secondary nodes mounted on a reindeer.

During the trials, two generators were used to power up secondary nodes, though it was noticed that the transmission was also achievable with just one generator. Communication ranges over 100 m were also observed in outdoors when the kinetic converter was activated because of the animal movement. Average data transmission rates of one frame every three minutes were estimated from the first results depending on the animal activity.

After the aforementioned tests, we needed to obtain different parameters on the network, such as the relationship between the secondary and primary reindeers, the GPS time acquisitions, or the number of base stations needed in a given area, for the correct working of the network in a real experiment. Therefore, we have developed a simulator (see Section 3) to extract these parameters and study the overall behavior of the network for the localization of live animals in this resource-constrained network.

### 3. Simulator

Our simulation platform is a fast, specialized simulator previously used for the study of swarm robotic behaviors [25]. It has a custom rigid body physics engine, specialized to simulate only the dynamics in environments containing flat terrain, obstacles and holes. This restriction allows for certain optimizations in the computation of the physics and thereby reduces the computational resources necessary for running simulations (see [26] for more details). Other simulators such as NS2, Opnet or OMNeT++ were considered as well as candidates for our research, but the current one was chosen because we found it more focused on our problem with shorter expected execution times. On the other hand, we expected the three aforementioned simulators to have support to run a wide range of network simulations which is good, but has drawbacks compared to the chosen specific solution.

In our simulation, a reindeer is modelled as a cylindrical body of 1.12 m diameter with a maximum speed of 2 km/h that holds primary or secondary nodes. Secondary nodes are made up of a radio link with a range up to 80 m and transmit statistically one frame each three minutes. Primary nodes are made up of a radio link with a range up to 600 m. GPS readings are obtained one per hour. In the secondary nodes, noise is added to the secondary–primary radio link. Each transmitted frame can be lost with a probability that varies linearly from 1% when the secondary–primary distance is less than 20 m to 70% when the two nodes are 80 m from each other.

### 4. Experiments

Forthcoming analysis and conclusions come from 24 experimental setups (ESs). Every ES consists of 200 nodes divided into primaries and secondaries nodes. Experiments are listed in Table 1. Reference names in Table 1 are made up by the base-station and primary-node number. Every experiment lasts for 15 simulation days – although the first 3 h are not accounted to avoid transient state – on a square area of  $4 \times 4 \text{ km}^2$  and node speed of 2 km/h. Secondary-node transmission pattern is uniformly distributed with a

**Table 1**  
Set of experiments run.

| Name    | Base stations | Primary $N$ | Secondary $N$ |
|---------|---------------|-------------|---------------|
| H1–20   | 1             | 20          | 180           |
| H1–40   | 1             | 40          | 160           |
| H1–60   | 1             | 60          | 140           |
| H1–80   | 1             | 80          | 120           |
| H1–100  | 1             | 100         | 100           |
| H1–120  | 1             | 120         | 80            |
| H4–20   | 4             | 20          | 180           |
| H4–40   | 4             | 40          | 160           |
| H4–60   | 4             | 60          | 140           |
| H4–80   | 4             | 80          | 120           |
| H4–100  | 4             | 100         | 100           |
| H4–120  | 4             | 120         | 80            |
| H5–20   | 5             | 20          | 180           |
| H5–40   | 5             | 40          | 160           |
| H5–60   | 5             | 60          | 140           |
| H5–80   | 5             | 80          | 120           |
| H5–100  | 5             | 100         | 100           |
| H5–120  | 5             | 120         | 80            |
| H16–20  | 16            | 20          | 180           |
| H16–40  | 16            | 40          | 160           |
| H16–60  | 16            | 60          | 140           |
| H16–80  | 16            | 80          | 120           |
| H16–100 | 16            | 100         | 100           |
| H16–120 | 16            | 120         | 80            |

mean of 180 s. At the beginning of the experiments all the reindeers are located in a circular area of 16 m radius considered as the nest. Once the experiment starts, all the reindeers follow a random walk for the 15 simulated days experiment duration.

Every base-station setup is depicted in Fig. 4 along with its coverage area. Unless the contrary is stated, the term *coverage area* refers to the area in which primary nodes

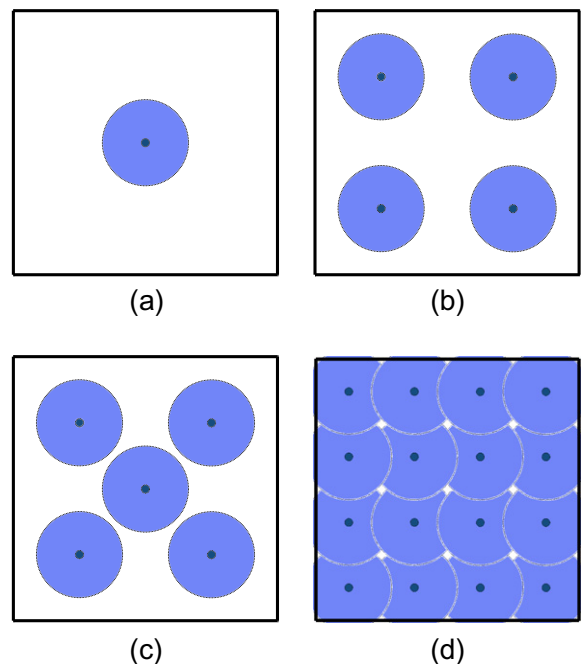


**Fig. 4.** Coverage area in H1(a), H4(b), H5(c) and H16(d).

can communicate with a base station: it is restricted by the radio link length. Other parameters will be detailed during the rest of the paper, as their knowledge is required to understand the results shown.

In subsequent sections, gamma and delta functions are used to characterize the probability distributions of three magnitudes. Delta is used because there are certain observations – localization delays – which happen on a specific time instant and their ratio over the complete set – probability – is proportional to a certain parameter ( $\alpha$ ). Gamma distribution was chosen because it is very flexible since both shape and scale can be controlled by means of two parameters. At the same time, we know that our three magnitudes on study are left side bounded and consequently such distribution fits very well such requirements. As a general form, the probability density function (PDF) of any magnitude can be expressed as:

$$f(\alpha, a, b, t) = \alpha\delta(t) + (1 - \alpha)f_r(t) \\ = \alpha\delta(t) + (1 - \alpha)\frac{b^{-a}}{\Gamma(a)}e^{-\frac{t}{b}}t^{a-1}, \quad t > 0 \quad (1)$$

and the cumulative distribution function (CDF) is:

$$F(\alpha, a, b, t) = \int_{-\infty}^t f(\alpha, a, b, t)dt, \quad (2)$$

in which  $\alpha$ ,  $a$  and  $b$  are specific parameters for every experiment and magnitude. For Localization events and Localization error alpha equals zero and therefore their PDF can be simplified as:

$$f(a, b, t) = \frac{b^{-a}}{\Gamma(a)}e^{-\frac{t}{b}}t^{a-1}, \quad t > 0 \quad (3)$$

Gamma function parameters ( $a, b$ ) are obtained from simulation outputs by means of their maximum likelihood estimators (MLEs) as it is defined in [27]:

$$\log \hat{a} - \psi(\hat{a}) = \log \left( \frac{\bar{t}}{\hat{b}} \right), \quad \hat{a}\hat{b} = \bar{t}, \quad (4)$$

$$\bar{t} = \frac{\sum_{i=1}^n t_i}{n} \quad \text{and} \quad \hat{t} = \left( \prod_{i=1}^n t_i \right)^{1/n}, \quad (5)$$

where  $\hat{a}$  and  $\hat{b}$  are the MLE of  $a$  and  $b$ ,  $t_i$  is the  $i$ th sample and  $n$  is the number of samples.

In the event that any output equals 0 – granularity is restricted to 0.1 s since it is a discrete time simulator – the method of matching moments (MM) recommended by Hahn and Shapiro [28] is computed rather than MLEs and gamma parameter expressions are:

$$\hat{b} = \frac{\sum_{i=1}^n (t_i - \bar{t})^2}{\bar{t}(n-1)}, \quad \hat{a}\hat{b} = \bar{t}. \quad (6)$$

Parameters  $a$ ,  $b$  and  $\alpha$  are detailed in every section along with the graphs of their associate functions – CDF and PDF. Every subsection corresponds to a magnitude and up to five descriptive indicators are provided: boxplots, histograms, adjusted PDFs, parameterized CDFs and values that match the 90th percentile. All are based on simulation outputs, PDFs and parameterized CDFs were obtained from

such outputs according to the aforementioned procedure – MLEs and MMs.

#### 4.1. Localization events

The term *localization event* means the number of localization events which have occurred for every secondary node, usually expressed over periods of 24 h. A localization event takes place when a primary node receives a secondary-node transmission and stores its last GPS reading, time and secondary's ID. That information is downloaded later on onto a base station when the base station 'appears' within the primary transmission range – the primary node gets enough close to a base station so that they can communicate. Fig. 5 sketches the box plots of a given base station configuration, all (24) are not drawn as results are similar and keep to the same trend as well: the number of base stations has a negligible impact on the number of localization events.

The primary-secondary ratio impacts on the system performance as it is observed from every subset of six experiments with a constant number of base stations: H1-x, H4-x, H5-x and H16-x. As long as such ratio increases so does the number of localization events. However, the number of primary nodes is what actually yields such variation. If one wishes to utilize a term more accurate, it would be better expressed as the number of primary nodes per area unit or primary-node-area ratio. The explanation is simple, a primary node behaves like an active beacon which monitors or covers a certain area (like a base station in a cellular system) at any given time. However, such a monitoring device moves and consequently its coverage area changes over time. *Active area* is the area within primaries' range and therefore, secondary nodes just candidate for being localized if they are in there. It will happen in the same fashion for any number of secondary nodes, i.e. localization events are independent of the number of secondary nodes. In the depicted experiments, area is constant (16 km<sup>2</sup>) but any individual may shortly deduce that any given number of primary nodes will not perform the same in environments with different sizes – although the active area will be the same, for a secondary node the probability of meeting any primary node will be lower

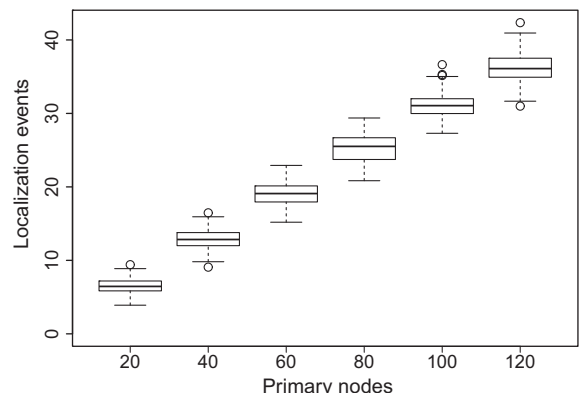


Fig. 5. Average of daily localization events per secondary node.

or higher and consequently the number of localization events. Therefore, the number of localization events depends on the number of primary nodes and size of the environment – the primary-area ratio.

As it has been already said, the localization-event distributions obtained from our simulations have been adjusted by means of (4) as gamma (3) CDFs. Table 2 shows the function parameters for the whole set of experiments. If one compares the sets of experiments row-wise, one realizes that  $a$  and  $b$  are nearly constant within each row – the same number of primary nodes – and therefore, their CDFs will be almost identical as shown in Fig. 6, which plots the CDF of every experiment. It shows better than any other graph the experiments grouped according to the number of primary nodes. Such function graphs overlap as it can be clearly observed for Hxx-20 and Hxx-40 and it is still noticeable for the other four.

Fig. 7 provides useful information in a glimpse on the system quality with respect to the localization events. For example, configurations with 20 primaries will enable a secondary node to be detected with 90% of probability at least 5 times per day. If the primary nodes are doubled (40) and tripled (60), a user will see any secondary at least 10 and 17 times, respectively. For setups with 80 and 100 primaries, such minimum rises as many as 22 and 29, respectively. The best case is obviously the one with greater primary–secondary ratio (for a given area) which in this analysis means 120 primaries and goes up to 33 localizations.

It is interesting to outline the linear relationship between localization events and number of primary nodes for any given set of experiments. As Table 3 shows, such ratio ( $N_{LE}/N_{LE20}$ ) keeps to a quantitatively similar trend to the rising number of primaries across the experiments of every set. Simulations are sorted by the primary–secondary ratio and for each both the mean ( $N_{LE}$ ) and ratio with respect to the corresponding Hx-20 experiment ( $N_{LE}/N_{LE20}$ ) are provided. The last column averages the former for every subset of constant primary–secondary ratio. Fig. 8 shows the aforementioned table graphically.

#### 4.2. Localization error

The *localization error* is defined as the absolute difference between a secondary node's actual position and the position stored on a primary node's records upon their encounter – i.e. a primary node is within a secondary node's transmission range by the time the latter is broadcasting.

**Table 2**

Localization-events gamma function parameters.

|     | H1     |      | H4     |      | H5     |      | H16    |      |
|-----|--------|------|--------|------|--------|------|--------|------|
|     | $a$    | $b$  | $a$    | $b$  | $a$    | $b$  | $a$    | $b$  |
| 20  | 43.17  | 0.15 | 43.3   | 0.15 | 43.16  | 0.15 | 43.26  | 0.15 |
| 40  | 91.65  | 0.14 | 91.41  | 0.14 | 91.49  | 0.14 | 91.99  | 0.14 |
| 60  | 143.62 | 0.13 | 146.94 | 0.13 | 147.86 | 0.13 | 145.8  | 0.13 |
| 80  | 160.56 | 0.16 | 165.72 | 0.15 | 160.53 | 0.15 | 166.18 | 0.15 |
| 100 | 302.47 | 0.1  | 313.27 | 0.1  | 314.12 | 0.1  | 317.93 | 0.1  |
| 120 | 261.11 | 0.14 | 268.53 | 0.13 | 269.82 | 0.13 | 270.78 | 0.13 |

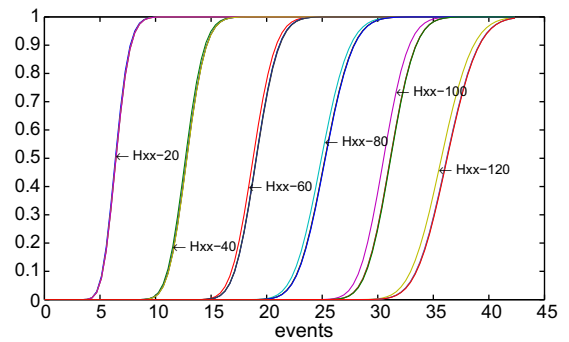


**Fig. 6.** Localization-events CDFs.

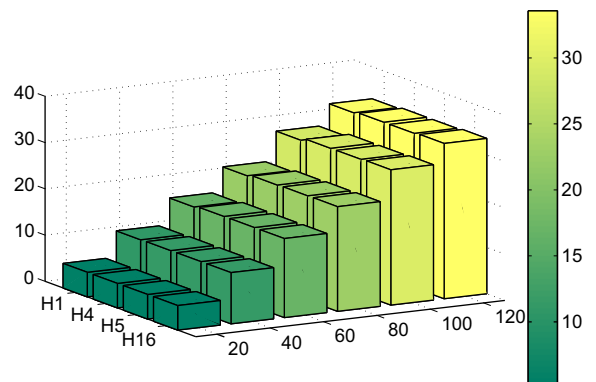


**Fig. 7.** Minimum number of localization events with 90% probability.

As the reader has already guessed, the most precise configuration for our system would be such that primary nodes represented 100% of the node population – secondaries would not have presence at all – GPS duty-cycle were 100% – in permanent operation – and a base station were within any primary's transmission range wherever the node were. Such configuration would let us reach nearly-instant updates of nodes' position and a negligible localization error which would merely depend on the GPS accuracy. Since our goal is to decrease the system cost to the extent that its performance still meets user's needs, attention is drawn to the localization error.

Boxplots are not shown as they are exactly the same across all the ESs. Two statistics are defined to represent medians and means of the localization error over all the ESs, namely  $L_{MED}$  and  $L_{AVG}$ . As every ES median is gathered

**Table 3**  
Localization events and primary nodes.

| Experiment set | Base stations | Loc. events – mean ( $N_{LE}$ ) | $N_{LE}/N_{LE20}$ | $E(N_{LE}/N_{LE20})$ |
|----------------|---------------|---------------------------------|-------------------|----------------------|
| Hx-20          | 1             | 6.42                            | 1                 | 1                    |
|                | 4             | 6.45                            | 1                 |                      |
|                | 5             | 6.45                            | 1                 |                      |
|                | 16            | 6.45                            | 1                 |                      |
| Hx-40          | 1             | 12.70                           | 1.98              | 1.99                 |
|                | 4             | 12.84                           | 1.99              |                      |
|                | 5             | 12.84                           | 1.99              |                      |
|                | 16            | 12.84                           | 1.99              |                      |
| Hx-60          | 1             | 18.86                           | 2.94              | 2.95                 |
|                | 4             | 19.09                           | 2.96              |                      |
|                | 5             | 19.13                           | 2.96              |                      |
|                | 16            | 19.13                           | 2.96              |                      |
| Hx-80          | 1             | 25.18                           | 3.92              | 3.95                 |
|                | 4             | 25.51                           | 3.95              |                      |
|                | 5             | 25.51                           | 3.95              |                      |
|                | 16            | 25.55                           | 3.96              |                      |
| Hx-100         | 1             | 30.52                           | 4.75              | 4.80                 |
|                | 4             | 31.06                           | 4.81              |                      |
|                | 5             | 31.06                           | 4.81              |                      |
|                | 16            | 31.09                           | 4.82              |                      |
| Hx-120         | 1             | 35.53                           | 5.53              | 5.58                 |
|                | 4             | 36.10                           | 5.59              |                      |
|                | 5             | 36.10                           | 5.59              |                      |
|                | 16            | 36.17                           | 5.60              |                      |

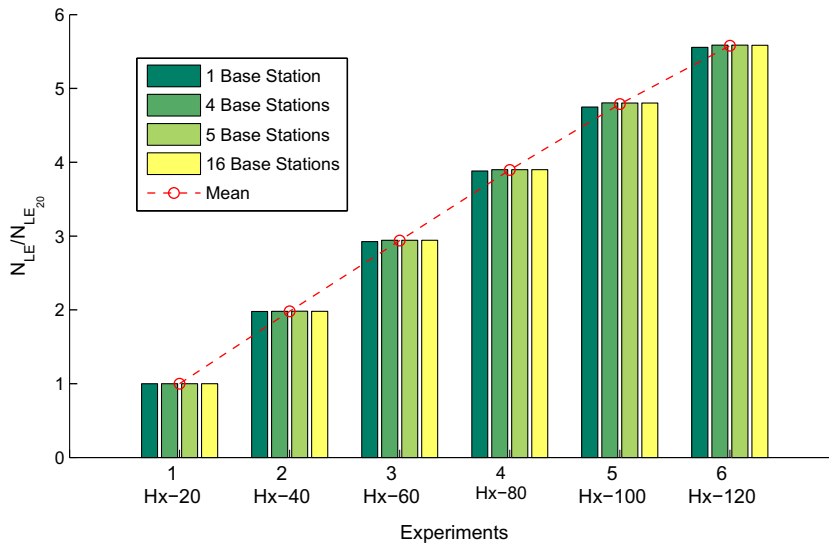


**Fig. 8.** Localization events normalized respect to 20 primary nodes.

in a set ( $L_{MED}$ ), one can observe that the mean ( $\mu$ ) of such set is very close to every element as it can be deduced from the low value of the coefficient of variation (CV).

**Table 4**  
Statistics of empirical medians and means of localization errors.

|           | $\mu$ (m) | CV     |
|-----------|-----------|--------|
| $L_{MED}$ | 611.47    | 0.0048 |
| $L_{AVG}$ | 666.13    | 0.0030 |

The same happens with the means ( $L_{AVG}$ ). Table 4 is intended to provide a better picture of the error invariance across the ESs (performance is nearly the same for any ES) by means its figures. Therefore, localization error is independent of the number of base stations, primary–secondary ratio or the size of the area. Since this metric is not linked to any information delay, but it is the result of a secondary–primary encounter along with the last GPS reading, mobility pattern and GPS duty-cycle determine the localization error.

$$E_{LOC-MAX} = D_p + D_{Tx-sec}. \quad (7)$$

The maximum localization error happens if both nodes are aligned with the spot where the primary node took the last GPS reading as depicted by Fig. 9.

Since the node speed is 2 km/h and GPS is switched on every hour, the maximum distance that a primary node can travel ( $D_p$ ) is 2 km while the maximum secondary transmission range ( $D_{Tx-sec}$ ) is 80 m. Hence the maximum localization error ( $E_{LOC-MAX}$ ) is 2.08 km. In addition, the means  $\mathbb{E}(L_{MED})$  and  $\mathbb{E}(L_{AVG})$  are 29% and 32% (see Table 4) of  $E_{LOC-MAX}$  which seems to be a promising performance compared to either the node speed and the worst case –  $E_{LOC-MAX}$ . Future work can be focused on studying the GPS duty-cycle along with the trade-off precision vs. primary-node lifetime. Moreover, further analysis on the effects of swarm mobility patterns on the system operation can lead to improve its performance.

As an example of CDF adjustment, Fig. 10 plots the histogram and the adjusted PDF for H4–80. PDF shapes are very similar – nearly the same – across all the experiments as one can infer from the parameters shown in Table 5. PDF is obtained according to (3) and its adjustment is computed by means of (4) as described earlier. From Fig. 11, a performance indicator can be outlined: the error is less than 1 km with 80% of probability, therefore in 80% of the observations the localization error is less than 1000 m which is less than half of the maximum possible: 2080 m. On the other hand, the 90th percentile (performance indicator common to the three magnitudes) ranges between 1232 and 1249 as shown in Fig. 12 – practically constant. A vast majority of observation errors will be less than 1250 m which is 40% less than the maximum theoretical error.

Consequently, as it was previously said, the localization error has no dependence on any other parameter but the GPS duty-cycle and the mobility pattern.

#### 4.3. Localization delay

The *localization delay* is the time elapsed from the instant on which a primary node detects a secondary node and the same primary node transmits that information to a base station, therefore system's awareness of a given localization event is not immediate or instantaneous. Depending on its characterization and user's requirements, system's implementation might be useless – if the delay were extremely high – or could pay off – for negligible or low values.

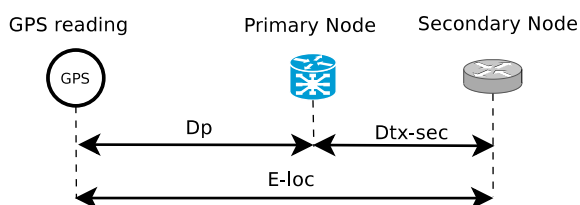


Fig. 9. Localization error.

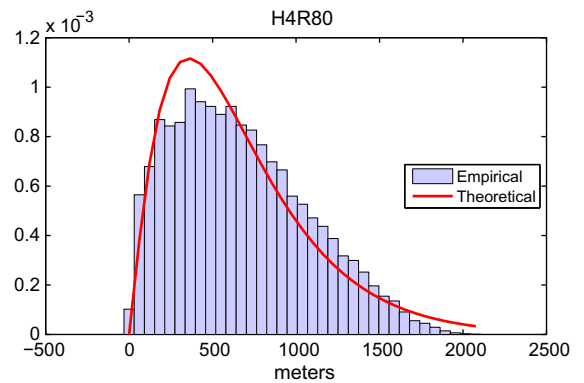


Fig. 10. Adjustment of localization-error PDF.

From Fig. 13 one realizes that the localization delay depends mainly on the number of base stations and much less on other factors such as primary–secondary ratio as it decreases as the number of base stations rises regardless the primary–secondary ratio. Median values shown as the 50th percentile mark on the box plots reinforce such statement as they are similar across the H1–xx experiments and steeply decreases with the number of base stations.

Let a base station be within a primary node's transmission range. When it happens, localization events have a transmission delay which is negligible. On real operation, a primary node is capable to transmit every 10 ms therefore, it has been modeled as instantaneous since the time granularity is the same one: 10 ms. All the localization events happened with a base station capable to receive and decode properly primary's signal have a zero transmission delay. Consequently, it is possible to segment the simulation area into two category sets: one of instant detection and another in which a localization delay is involved. Fig. 4 shows specifically such areas which are circles whose radius is the primary transmission range: 600 m. In H1, H4 and H5 experiments are disjoint, while in H16 they overlap as the distance between base stations is shorter than the double of the aforementioned transmission distance: 1000 m.

The observations obtained across the 24 ESs show a number of them concentrated on  $t = 0$ . Such observations take place within the colored areas depicted in Fig. 4 and their number increases as these areas become larger. Therefore, such phenomenon will be much more noticeable in H16-xx than in H1-xx; H4-xx and H5-xx will fall in between. Since the mobility pattern is a random walk (or semi-random if one allows for the fact that nodes cannot traverse simulation boundaries) a given node's presence is equally probable for all the points which make up the simulation area over the whole simulation. Consequently, there should be a relationship between the amount of events instantly detected and the colored area. In fact, it is linked to the quantitative relationship between the coverage area over the simulation area. For H1, H4 and H5 ESs it is straight to calculate it as the summation of every base-station coverage area. In H16-xx, it is better to do it from the non-covered area. Such information is the alpha parameter referred in the table below and shows

**Table 5**  
Error gamma function parameters.

|     | H1   |        | H4   |        | H5   |        | H16  |        |
|-----|------|--------|------|--------|------|--------|------|--------|
|     | a    | b      | a    | b      | a    | b      | a    | b      |
| 20  | 2.14 | 309.67 | 2.14 | 309.37 | 2.14 | 309.32 | 2.14 | 309.38 |
| 40  | 2.17 | 305.93 | 2.17 | 306.02 | 2.17 | 306    | 2.17 | 306.04 |
| 60  | 2.16 | 308.67 | 2.16 | 308.29 | 2.16 | 308.25 | 2.16 | 308.28 |
| 80  | 2.15 | 309.91 | 2.15 | 310.2  | 2.15 | 310.17 | 2.15 | 310.28 |
| 100 | 2.16 | 310.27 | 2.15 | 310.75 | 2.15 | 310.85 | 2.15 | 310.75 |
| 120 | 2.17 | 307.95 | 2.17 | 308.06 | 2.17 | 308.05 | 2.17 | 308.07 |

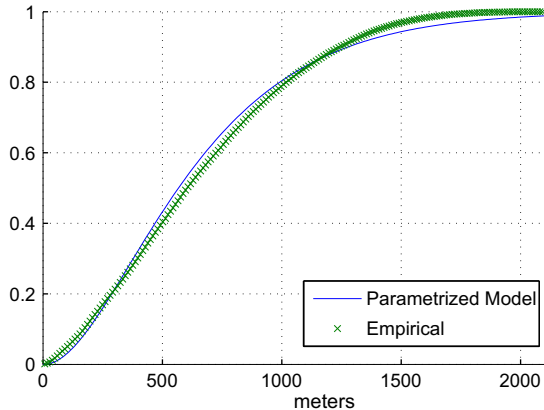


**Fig. 11.** Empirical and parameterized error CDFs.

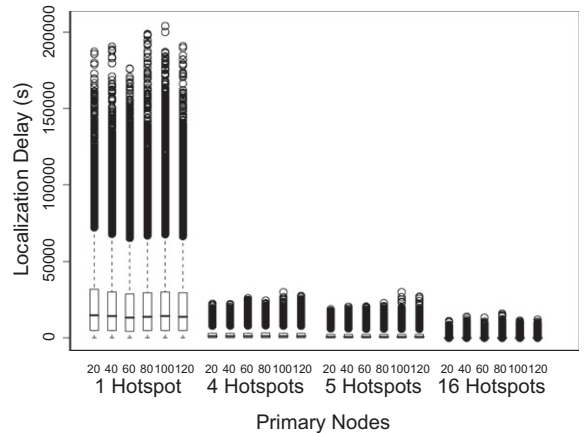


**Fig. 13.** Localization delay.

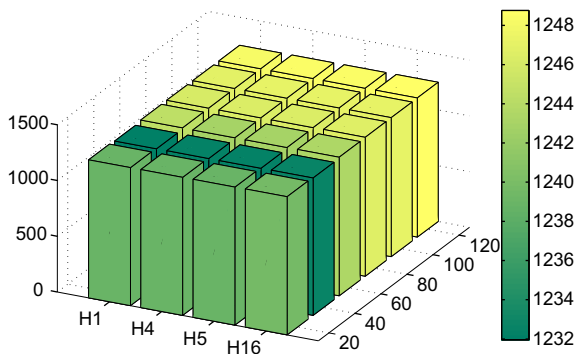


**Fig. 12.** Maximum error (m) with 90% probability.

how the coverage area ratio is nearly 100% in H16-xx, around 35% in H5, 28% in H4 experiments and 7% for the one-base-station case.

Upon modeling the empirical results obtained from the simulations, it was decided to split the observations into two groups: a number of them equal to zero and proportional to the alpha parameter and the rest which were adjusted by means of (4) and (6) as gamma distributions (1). Gamma parameters are similar across the experiments, though not exactly the same. As Table 6 shows, they can be grouped according to the number of base stations. For gamma distributions,  $b$  parameter is known as the scale parameter which is meaningful in this case as it gives an

idea on the magnitude order: H1  $b$ 's are around ten times greater than H4  $b$ 's and H5  $b$ 's are even lower. It can be explained from the fact that any primary node which is not *in touch* with a base station has to traverse less distance to reach the coverage area as the number of base stations rises. A similar trend can be observed in the performance metric detailed in this section.

Fig. 14 shows the CDFs of the experiments H1, H4 and H5. H16's are not shown as the probability is 1 for any time. In the former ones, function graphs show clearly the effect of the  $\delta$  function since the graphs start near (0,0.07) for H1's, (0,0.3) for H4's and (0,0.35) for H5's. The ordinate corresponds to  $\alpha$  in Eq. (1) and it amounts to the values given in Table 6. The quantitative difference between H1's and H4's can be observed in a number of details besides the mere function shape, thus nearly 100% of H4 observations fall below  $10^4$  s while H1's are upper bounded by  $12 \cdot 10^4$  s and less than 40% of their observations fall below  $10^4$  s.

One can obtain a more intuitive idea of the performance regarding the localization delay from Fig. 15 which shows the 90th percentile for every experiment. Once again, it is obvious that H1 delays are higher than H4's and H5's.

The same performance metric as in previous magnitudes is applicable in this case. H1-xx configurations are upper bounded by the interval [49,686,55,435] ( $\sim 14$  h), H4-xx's go steeply to nearly one tenth [5659,5715] ( $\sim 1$  h 35') while H5-xx's even lower to [4523,4591] ( $\sim 1$  h 16') and it becomes null in the event that 16 base stations are deployed.

**Table 6**  
Delay function parameters.

| $\alpha$ | H1   |          | H4   |         | H5   |         | H16  |         |
|----------|------|----------|------|---------|------|---------|------|---------|
|          | 0.07 |          | 0.28 |         | 0.35 |         | 0.96 |         |
|          | $a$  | $b$      | $a$  | $b$     | $a$  | $b$     | $a$  | $b$     |
| 20       | 0.94 | 26,671   | 1.18 | 2544.56 | 1.1  | 2259    | 0.62 | 2233.07 |
| 40       | 0.99 | 23186.1  | 1.15 | 2631.59 | 1.06 | 2381.2  | 0.61 | 2341.63 |
| 60       | 0.95 | 23405.65 | 1.15 | 2645.75 | 1.07 | 2310.94 | 0.64 | 1929.43 |
| 80       | 0.97 | 23510.94 | 1.14 | 2648.05 | 1.04 | 2406.52 | 0.62 | 2189.7  |
| 100      | 0.98 | 23630.77 | 1.11 | 2680.9  | 1.04 | 2372.47 | 0.65 | 1996.17 |
| 120      | 1    | 22515.68 | 1.09 | 2765.28 | 1.04 | 2383.91 | 0.62 | 2078.58 |

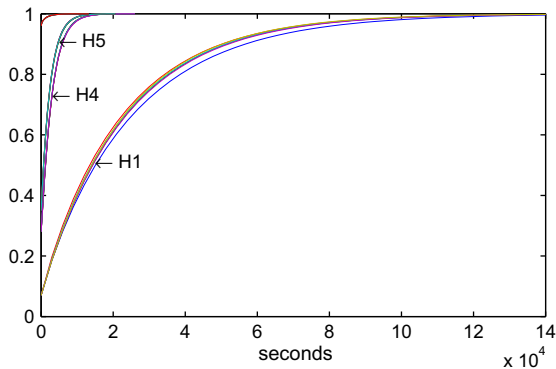


**Fig. 14.** Delay CDFs.

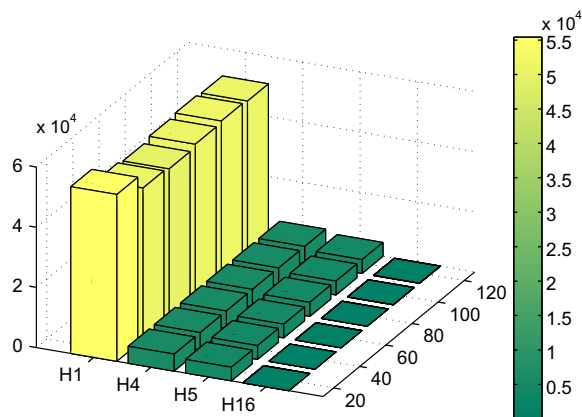


**Fig. 15.** Maximum localization delay with 90% probability.

Localization delay is not generally coupled to other magnitudes' performance as long as the application environment is defined (which consequently spans a mobility pattern) since it is an inherent delay from the time a localization event happens to the time the system is informed of its occurrence. As it is pointed out, it depends on the base-station coverage area and mobility pattern which are restricted indeed to the coverage area as the mobility pattern is constrained by the application environment. Consequently, the system delay can be adjusted despite of any other magnitude or parameter, but simply the ratio between the coverage-area and the total-area as the oper-

ational framework is given. Otherwise, it can be considered indirectly linked to other parameters by the node mobility.

#### 4.4. Primary–secondary ratio

Previous sections on localization magnitudes have sketched a reasoning which leads to the conclusion that the primary–secondary ratio has a negligible impact on the overall localization performance. However, since previous experiments had a fixed total population (i.e., 200 individuals), one might suspect that there would still be an impact from such ratio.

In order to test the scalability and robustness of the system, we run another set of experiments with a variable node population – primary-node number being invariant (60) and secondary-node being variable: 30, 60, 100, 150 and 300. For every experiment the arena is the same as before ( $4 \times 4 \text{ km}^2$ ), there are 4 base stations and simulation time lasts 7 days.

The localization delay and localization error parameters are within the expected range. For the former, we observe that the  $a$  and  $b$  parameters (see Table 7) are similar to the previous experiments shown in Table 6, column H4. Results for the localization error show a similar performance if comparing Table 7 with Table 5, column H4. Localization events parameters (i.e.  $a$  and  $b$ ) differ slightly from their homologous in Table 2, which may be because of the limited number of samples (30 to 300). However, Table 7 shows the means of localization events for the new experiments; if they are compared with the means for Hx-60 experiments (Table 3, third column ( $N_{LE}$ )) the reader may see that they are the same. Fig. 16 shows clearly the fact that distributions are similar for the same number of primary nodes regardless of the amount of secondary nodes. Experiments labeled as 20–180, 40–160, 60–140, 80–120 and 100–100 correspond to the previous experiments

**Table 7**  
Gamma function parameters for the experiments with a fixed primary node population.

|     | Delay |         | Error |        | Loc. events |      |       |
|-----|-------|---------|-------|--------|-------------|------|-------|
|     | $a$   | $b$     | $a$   | $b$    | $a$         | $b$  | $\mu$ |
| 30  | 1.13  | 2685.47 | 2.20  | 300.46 | 83.29       | 0.23 | 19.20 |
| 60  | 1.11  | 2677.92 | 2.15  | 310.37 | 75.47       | 0.26 | 19.43 |
| 100 | 1.10  | 2719.52 | 2.16  | 308.31 | 51.90       | 0.37 | 18.96 |
| 150 | 1.15  | 2628.79 | 2.14  | 311.44 | 63.26       | 0.30 | 19.25 |
| 300 | 1.13  | 2651.05 | 2.17  | 308.39 | 60.79       | 0.31 | 18.68 |

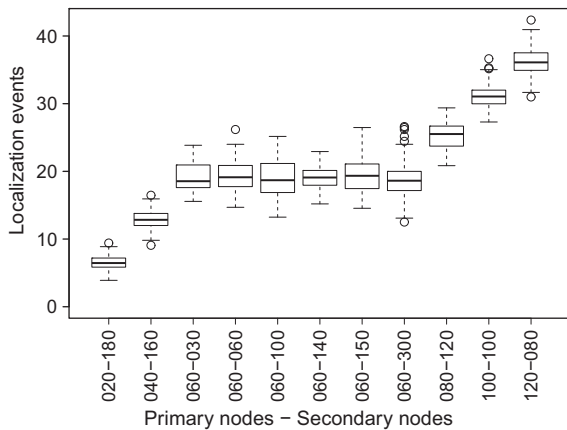


Fig. 16. Comparison of the daily localization events per secondary node for all the experiments with four base stations.

described in Table 1 with 4 base stations (H4-xx) and labels 60–30, 60–60, 60–100, 60–150 and 60–300 are the extra experiments for the present subsection. Therefore, we can finally conclude that primary–secondary ratio does not impact at all on the overall localization performance.

## 5. Conclusions

The performance of our system has turned out to be more complex than expected initially as not just one operational parameter defines its behavior. Consequently, our system is more adaptive to a vast variety of environments and applications. Therefore, rather than pointing out an optimal configuration which fulfills user's needs for most cases, it is necessary to define the operational environment, costs and desired performance for every given case to check – based on the mathematical adjustment and simulations – its feasibility or deviation from the targeted case.

It should be outlined once again the fact that there is no need to have a GPS device to monitor a mobile node (usually an animal) if one allows for a rough localization whose accuracy will depend on the system configuration. GPS duty-cycle and mobility pattern are out of the scope of the present paper, but they will be part of future work as parameters such as localization error, localization events, time between localizations and even delay depend directly or indirectly on them.

As it has been shown, the active area (which was defined as the primary node-area ratio) determines the number of *localization events* per secondary node. Depending on the user's requirements, more or less primary nodes will be necessary and consequently the deployment will be cheaper or more expensive. Note that a primary node cost is much higher than a secondary one simply for the sake of integrating a GPS device and a battery which do not exist on a secondary board. Anyway, it is generally cost saving compared to a configuration with one GPS device per individual (animal) to be localized. At first, a configuration with 30% of primaries (Hx-60) seems reasonable to keep track of a node's presence for the herding purposes previ-

ously detailed as it would be at least 17 times per day. Such figures mean at least a maximum timing between localizations of 3.5 h.

*Localization error* is a key feature in any localization system and therefore of major interest. In the system on study, such metric is mainly determined by the GPS duty-cycle. One might decide happily to raise it in order to decrease such a magnitude, but its variation will be constrained by the operating conditions. In addition, error is not sometimes the unique demanded feature as any given user may require longer unattended operation for a number of reasons such as the operating temperature, which may be very low affecting batteries performance, a mandatory low cost of maintenance or any other that can come up as it can be considered a general-purpose system for rough localization. Anyway, it is very promising that the maximum error reached with 90% of probability across the 24 ESs is 1250 m and 80% of the localizations are more accurate than 1 km while the GPS device is just turned on once per hour. It must be taken into account the fact that for such duty cycle (once per hour) a primary node powered with 4 regular alkaline AA batteries should span its lifetime 3 or 6 months for  $-20\text{ }^{\circ}\text{C}$  to  $+15\text{ }^{\circ}\text{C}$  operation temperatures. Future work will focus on this topic.

The number of base stations would be ideally such that there were no area out of the reception range of any of them, however, there are a two drawbacks related to the deployment of such stations: their cost and their environmental impact. Therefore, a trade-off between cost, environmental impact and delay requirements is necessary for every deployment. Moreover, the mobility pattern has not been mentioned so far as it is considered a constant in our simulations, but obviously has some influence on the time that primary nodes spend to 'go back' (*localization delay*) to a base station from a localization event.

Ideally, one might wish to monitor every single node movement with as much granularity as possible and to be informed instantly of every update. However, there is a number of pros and cons already described through the current paper. Delay can be reduced to almost zero if the number of base stations is raised enough, however such deployment can be limited by environmental regulations or costs. On the other hand, shorter GPS duty cycles will diminish system error, though they may lead to shorten the battery lifetime and as a consequence raise maintenance costs. Something similar happens with the active area which determines the number of localization events as well as the time elapsed between localizations: the higher it is, the better the system will perform, however it means more primary nodes and therefore higher deployment costs compared to using secondary nodes.

If a certain setup had to be chosen, one with around 30% or 40% coverage area (H4-xx or H5-xx) could provide a reasonable delay ( $\sim 1.5$  h) compared to the time between localizations (3.5 h) imposed by 30% of primary–secondary (Hx-60). In such case (H4), the minimum localization-event number would be 17. Overall, such configuration ( $\sim$ H4–60) seems to be quite cheaper than another one with 16 base stations (H16-xx – 100% coverage area) or 50/50 node ratios (Hx-100). Compared to H1 configurations it has the advantage of dramatically decreasing the

delay with just two or three more base stations. If one takes into account that a base station is *simply* a board with an enclosure and a battery, one may conclude that in most cases it can be acceptable to deploy three or four in 16 km<sup>2</sup> – like the simulation area.

## Acknowledgments

The authors acknowledge support from RBZ Robot Design S.L. Company. This work has been sponsored by the Community of Madrid and the European Social Fund, the 7th Framework ICT project N4C – Networking for Challenged Communications Citizens: Innovative Alliances and Test beds project (FP7-ICT-223994-N4C) which is partly funded by the European Union and partly by the Spanish Science and Innovation Ministry under the complementary action Grant TEC 2008-04644-E. Other Grants supporting this work are CSD2008-00010 COMONSENS, FP7-ICT-2009-4-248894, TEC2009-14219-C03-01, TEC2007-67520-C02-01/02/TCM and TSI-020400-2009-20.

## References

- [1] J.M. Kahn, R.H. Katz, K.S.J. Pister, Next century challenges: mobile networking for ‘smart dust’, in: Proceedings of the 5th Annual ACM/IEEE International Conference on Mobile Computing and Networking, ACM Press, New York, NY, 1999, pp. 271–278.
- [2] K. Fall, S. Farrell, DTN: an architectural retrospective, *Selected Areas in Communications* 26 (5) (2008) 828–836.
- [3] S. Farrell, V. Cahill, Delay- and Disruption-Tolerant Networking, Artech House, Boston, MA, 2006.
- [4] A. Balasubramanian, B. Levine, A. Venkataramani, DTN routing as a resource allocation problem, in: Proceedings of the 2007 Conference on Applications, Technologies, Architectures and Protocols for Computer Communications, ACM Press, New York, NY, 2007, pp. 373–384.
- [5] S. Burleigh, V. Cerf, R. Durst, K. Fal, A. Hooke, K. Scott, H. Weiss, The interplanetary internet: a communications and infrastructure for mars, in: Proceedings of the 53rd International Astronautical Congress, The World Space Congress, International Astronautical Federation, Paris, France, 2002.
- [6] V. Cerf, S. Burleigh, A. Hooke, L. Torgerson, R. Durst, K. Scott, K. Fall, H. Weiss, Delay-tolerant networking architecture, Tech. Rep. RFC 4838, Jet Propulsion Laboratory, Pasadena, CA, 2007.
- [7] N4C project website. Available from: <<http://www.n4c.eu/>>.
- [8] A. Gutiérrez, C. González, J. Jiménez-Leube, S. Zazo, N. Dopico, I. Raos, A heterogeneous wireless identification network for the localization of animals based on stochastic movements, *Sensors* 9 (5) (2009) 3942–3957.
- [9] J. Hightower, G. Borriello, Location systems for ubiquitous computing, *Computer* 34 (8) (2001) 57–66.
- [10] C.D. Kidd, R. Orr, G.D. Abowd, C.G. Atkeson, I.A. Essa, B. MacIntyre, E.D. Mynatt, T. Starner, W. Newstetter, The aware home: a living laboratory for ubiquitous computing research, in: Proceedings of the Second International Workshop on Cooperative Buildings, Integrating Information, Organization, and Architecture, Springer-Verlag, 1999, pp. 191–198.
- [11] A. Doria, M. Uden, D.P. Pandey, Providing connectivity to the saami nomadic community, in: Proceedings 2nd International Conference on Open Collaborative Design for Sustainable Innovation, 2002.
- [12] M. Taillade, Trends in satellite-based animal tracking, in: P. Macini, S. Fioretti, C. Cristalli, R. Bendini (Eds.), *Biotelemetry*, vol. XII, Litografia Felici, Pisa, Italy, 1993, pp. 291–297.
- [13] F. Papi, P. Luschi, R. Crosio, G.R. Hughes, Satellite tracking experiments on the navigational ability and migratory behaviour of the loggerhead turtle *Caretta*, *Marine Biology* 129 (2) (1997) 215–220.
- [14] M.C. Perry, D.M. Kidwell, A.M. Wells-Berlin, E.J.R. Lohnes, G.H. Olsen, P.C. Osenton, Habitats used by black and surf scoters in eastern north american as determined by satellite radio telemetry, in: Second North American Sea Duck Conference, Patuxent Wildlife Research Center, Laurel, MA, 2005, pp. 21–35.
- [15] L.D. Rosa, E.R. Secchi, Y.G. Maia, A.N. Zerbini, M. Heide-Jorgensen, Movements of satellite-monitored humpback whales on their feeding ground along the antarctic peninsula, *Polar Biology* 31 (7) (2008) 771–781.
- [16] R. Vijay, A. Kansal, J. Friedman, S. Mani, Design consideration for solar energy harvesting wireless embedded systems, in: Proceedings of the IEEE International Conference on Information Processing and Sensor Networks, IEEE Press, Piscataway, NJ, 2005, pp. 457–462.
- [17] H. Ritter, J. Schiller, T. Voigt, A. Dunkels, J. Alonso, Experimental evaluation of lifetime bounds for wireless sensor networks, in: Proceedings of the Second European Workshop on Wireless Sensor Networks, IEEE Press, Piscataway, NJ, 2005, pp. 25–32.
- [18] P. Zhang, C.M. Sadler, S.A. Lyon, M. Martonosi, Hardware design experiences in zebranet, in: Proceedings of the Second International Conference on Embedded Networked Sensor Systems, ACM Press, New York, NY, 2004, pp. 227–238.
- [19] Turtlenet project website. Available from: <<http://prisms.cs.umass.edu/dome/turtlenet/>>.
- [20] N.S. Shenck, J.A. Paradiso, Energy scavenging with shoe-mounted piezoelectrics, *IEEE Micro* 21 (3) (2001) 30–42.
- [21] T. Starner, Human-powered wearable computing, *IBM Systems Journal* 35 (3) (1996) 618–629.
- [22] J.A. Paradiso, M. Feldmeier, A compact, wireless, self-powered pushbutton controller, in: Proceedings of the third International Conference on Ubiquitous Computing, Springer-Verlag, Berlin, Germany, 2001, pp. 299–304.
- [23] C. Partk, P.H. Chou, Ambimax: autonomous energy harvesting platform for multi-supply wireless sensor nodes, in: Proceedings of the Third Annual Conference of IEEE Communications Society on Sensor and Ad Hoc Communications and Network, IEEE Press, Piscataway, NJ, 2006, pp. 168–177.
- [24] R. Want, An introduction to rfid technology, *IEEE Pervasive Computing* 5 (1) (2006) 1–25.
- [25] A. Gutiérrez, A. Campo, F.C. Santos, F. Monasterio-Huelin, M. Dorigo, Social odometry: imitation based odometry in collective robotics, *International Journal of Advanced Robotic Systems* 6 (2) (2009) 129–136.
- [26] A.L. Christensen, Efficient neuro-evolution of hole-avoidance and phototaxis for aswarm-bot, Tech. Rep. 2005-014, IRIDIA, Université Libre de Bruxelles, Brussels, Belgium, 2005.
- [27] J.F. Lawless, *Statistical Models and Methods for Lifetime Data* (Wiley Series in Probability & Mathematical Statistics), John Wiley & Sons, 1982. Available from: <<http://www.worldcat.org/isbn/0471085448>>.
- [28] G.J. Hahn, S.S. Shapiro, *Statistical Models in Engineering*, John Wiley & Sons, 1967.



**Nelson Dopico** received a MS. degree, in 2005, and BS. degree, in 2003, in Telecommunications Engineering from the Universidad Politécnica de Madrid (UPM), Spain. Between 2003 and 2005 worked as a software developer. Since 2006, he is a research assistant at the Department of Signals, Systems and Radio communications of UPM. He was a visiting researcher at Trinity College Dublin in 2009. His research interests include wireless sensor networks, delay tolerant networks and WSN architectures.

**Álvaro Gutiérrez** received the M.Sc. degree in Electrical Engineering in 2003 and the Ph.D. degree in Computer Science in 2009 both from the Universidad Politécnica de Madrid (UPM), Madrid, Spain. In 2008 he was a Visiting Researcher at the Institute de Recherches Interdisciplinaires et de Développements en Intelligence Artificielle (IRIDIA) at the Université Libre de Bruxelles (ULB), Belgium. He is currently an Assistant Professor of automatic and control systems at the ETSI Telecomunicación of the UPM. He has authored and coauthored three book chapters and more than 20 refereed journals papers and conference proceeding papers. His research interests include swarm robotics, control systems, sensors networks and demand-side management applications especially focused on smart-grids and renewable energies.

**Santiago Zazo** is Telecom Engineer and Dr. Engineer by the Universidad Politécnica de Madrid (UPM) in 1990 and 1995 respectively. From 1991–1994 he was with the University of Valladolid and from 1995–1997 with

the University Alfonso X El Sabio in Madrid. In 1998 he joined UPM as Associate Professor in Signal Theory and Communications. His main research activities are in the field of Signal Processing with applications to Audio, Communications and Radar. More recently, he has been mostly focused on MIMO communications and Wireless Sensor Networks from both physical layer and networking points of view. Since 1990 he is

author/coauthor of more than 10 journal papers and about 90 conference papers. He has also led many private and national Spanish projects and has participated in five European projects, leading three of them. He is leading the HF communication group at UPM with large activity in publications and technological transfer to civil and military applications in this field.